Published in final edited form as:
J Immunol. 2011 December 1; 187(11): 5813–5823. doi:10.4049/jimmunol.1101068.

Peptidoglycan Recognition Protein Pglyrp2 Protects Mice from Psoriasis-Like Skin Inflammation by Promoting Treg and Limiting Th17 Responses*

Shin Yong Park[‡], **Dipika Gupta**[‡,¶], **Risa Hurwich**[‡], **Chang H. Kim**[§], and **Roman Dziarski**[‡,¶]
[‡]Indiana University School of Medicine–Northwest, Gary, IN 46408, USA
[§]School of Veterinary Medicine, Purdue University, West Lafayette, IN 47907, USA

Abstract

Skin protects the body from the environment and is an important component of the innate and adaptive immune systems. Psoriasis is a frequent inflammatory skin disease of unknown etiology determined by multigenic predisposition, environmental factors, and aberrant immune response. Peptidoglycan Recognition Proteins (Pglyrps) are expressed in the skin and we report here that they modulate sensitivity in an experimentally-induced mouse model of psoriasis. We demonstrate that *Pglyrp2*$^{-/-}$ mice (but not *Pglyrp3*$^{-/-}$ and *Pglyrp4*$^{-/-}$ mice) are more sensitive to the development of 12-O-tetradecanoylphorbol 13-acetate (TPA)-induced psoriasis-like inflammation, whereas *Pglyrp1*$^{-/-}$ mice are less sensitive. The mechanism underlying this increased sensitivity of *Pglyrp2*$^{-/-}$ mice to TPA-induced psoriasis-like inflammation is reduced recruitment of Treg cells to the skin and enhanced production and activation of Th17 cells in the skin in *Pglyrp2*$^{-/-}$ mice, which results in more severe inflammation and keratinocyte proliferation. Thus, in wild type mice, Pglyrp2 limits over-activation of Th17 cells by promoting accumulation of Treg cells at the site of inflammation, which protects the skin from the exaggerated inflammatory response.

Introduction

The innate immune system not only protects the host from infections, but it also responds to tissue damage and environmental chemicals (including allergens), and it initiates adaptive immune responses. Skin protects the body from the environment and is the largest organ in mammals. Besides forming a mechanical barrier, skin is an important component of the innate and adaptive immune systems rich in anti-microbial peptides and antigen-sensing cells, and it maintains the proper homeostatic balance between pro- and anti-inflammatory responses. Psoriasis is one of the most frequent inflammatory skin diseases in western societies. Psoriasis has a prevalence of 2–4% and is manifested by areas of epidermal overgrowth and scaling. The etiology of psoriasis is unknown and it is determined by multigenic predisposition, environmental factors, and aberrant immune response (1,2). Psoriasis does not develop spontaneously in animals, and thus there is a need for experimental animal models of psoriasis that can be used to dissect its etiology and pathogenesis, and to develop and evaluate new therapies.

One class of innate immunity proteins expressed in the skin are Peptidoglycan Recognition Proteins (PGRPs or Pglyrps). PGRPs are conserved from insects to mammals, recognize bacterial peptidoglycan, and function in antibacterial immunity. Mammals have four PGRPs,

*This work was supported by USPHS Grants AI028797 and AI073290 from NIH.

¶Correspondence: dgupta@iun.edu or rdziar@iun.edu, Tel 219-980-6535, Fax 219-980-6566.

Pglyrp1, Pglyrp2, Pglyrp3, and Pglyrp4, which were initially named PGRP-S, PGRP-L, PGRP-Iα, and PGRP-Iβ, respectively (3,4). Pglyrp1, Pglyrp3, and Pglyrp4 are directly bactericidal (5–8), whereas Pglyrp2 is an N-acetylmuramoyl-L-alanine amidase that hydrolyzes peptidoglycan (9,10). Pglyrp1 is highly expressed in PMN's granules and to a much lower extent in other cells (4,11,12). Pglyrp2 is constitutively expressed in the liver, from which it is secreted into blood, and Pglyrp2 expression is induced in keratinocytes and other epithelial cells (9,10,13–17). Different transcription factors control constitutive and inducible expression of Pglyrp2 (17). Pglyrp3 and Pglyrp4 are highly expressed in the skin and are also expressed in the salivary glands, throat, tongue, esophagus, stomach, intestine, and eyes (5,18,19).

In vivo, mammalian PGRPs protect mice against experimental colitis (19), but at least one PGRP (Pglyrp2) has an opposite proinflammatory effect in a model of experimental arthritis (20). We hypothesized that PGRPs play a role in the development of psoriasis because of (a) the prominent expression of PGRPs in the skin, (b) their ability to modulate the sensitivity to colitis and arthritis (19,20); (c) the location of *Pglyrp3* and *Pglyrp4* genes in the epidermal differentiation gene cluster in the psoriasis sensitivity *psors4* locus, (d) coordinated expression of *Pglyrp3* and *Pglyrp4* with other genes in the *psors4* locus, and (e) previous evidence of genetic association of *Pglyrp3* and *Pglyrp4* variants with psoriasis (21,22). Here we tested this hypothesis using PGRP-deficient mice and a mouse model of chemically-induced psoriasis-like inflammation.

We demonstrate that *Pglyrp2*$^{-/-}$ mice (but not *Pglyrp3*$^{-/-}$ and *Pglyrp4*$^{-/-}$ mice) are more sensitive to the development of experimental psoriasis-like inflammation, whereas *Pglyrp1*$^{-/-}$mice are less sensitive than wild type (WT) mice. The mechanism underlying this increased sensitivity of *Pglyrp2*$^{-/-}$ mice is reduced recruitment of Treg cells to the skin and enhanced production and activation of Th17 cells in *Pglyrp2*$^{-/-}$ mice, which results in more severe inflammation and keratinocyte proliferation. Thus, in WT mice, Pglyrp2 limits over-activation of Th17 cells by promoting accumulation of Treg cells at the site of inflammation, which protects the skin from the exaggerated inflammatory response.

Materials and Methods

Mice

We generated *Pglyrp1*$^{-/-}$, *Pglyrp2*$^{-/-}$, *Pglyrp3*$^{-/-}$, and *Pglyrp4*$^{-/-}$ mice as described previously (12,19,20). We generated *Pglyrp1*$^{-/-}$*Pglyrp2*$^{-/-}$, *Pglyrp1*$^{-/-}$*Pglyrp3*$^{-/-}$, and *Pglyrp2*$^{-/-}$*Pglyrp3*$^{-/-}$ double knockout mice and *Pglyrp1*$^{-/-}$*Pglyrp2*$^{-/-}$*Pglyrp3*$^{-/-}$ triple knockout mice by breeding single and double knockout mice (all on BALB/c background) and screening for homozygous deletion of each *Pglyrp* gene by PCR analysis of genomic DNA as previously described (12,19,20). The lack of expression of the *Pglyrp* genes was confirmed by qRT-PCR in mRNA from the ears. Double and triple homozygous *Pglyrp* knockout mice were viable and fertile, bred normally, and yielded the expected male:female ratios and similar litter size as the wild type and heterozygous mice. They had similar weight as the WT and single *Pglyrp* knockout mice and developed normally with no obvious defects. Their major internal organs had normal macroscopic appearance, and normal histological appearance on hematoxylin/eosin-stained sections.

All mice used in experiments were 8–10 week-old and on BALB/c background. The original colony founder WT BALB/c breeder mice were obtained from Harlan-Sprague-Dawley. All knockout mice were backcrossed to the same WT BALB/c mice from our breeding colony, and all WT and knockout mice were bred and kept under conventional pathogen-free conditions in the same room in our facility to minimize the influence of differences in the environment. For each experiment, mice from several different cages and breeder pairs were

used. The BALB/c background of *Pglyrp*-deficient mice and their negative status for all common viral and bacterial pathogens and parasites were confirmed as previously described (19). All experiments on mice were approved by the Indiana University School of Medicine–Northwest Institutional Animal Care and Use Committee.

TPA-induced psoriasis-like inflammation model

20 μl of 0.01% TPA (12-O-tetradecanoylphorbol 13-acetate, Sigma, in 2% DMSO, 98% acetone) was applied to each ear (10 μl to each side) of male mice on days 0, 2, 4, 6, and 8 (23). Ear thickness was measured each time before TPA application with Digimatic Micrometer (Mitutoyo, Japan) under constant pressure at the lowest setting. Ear swelling was determined by subtracting the untreated ear thickness (day 0). The significance of differences in ear swelling was determined using *t*-test.

Histology

For histological analysis ears were fixed in Bouin's fixative, postfixed in 70% ethanol, and embedded in paraffin, and cross-sections were stained with hematoxylin/eosin, and evaluated microscopically. Histologic changes (acanthosis, formation of rete pegs, parakeratosis, parakeratotic scaling, thickening of the sub-epidermal layer, cellular infiltration) were evaluated semi-quantitatively on a scale of 0 to 6 (0 = no change from untreated ears; 6 = maximum change in treated ears). The surface areas of microabscesses on cross-sections were measured using ImageJ software from NIH.

RNA and quantitative real-time reverse transcription PCR (qRT-PCR)

RNA was isolated from either the entire untreated or treated ears or cervical lymph nodes using the TRIZOL method (InVitrogen), followed by digestion with RNase-free DNase (Qiagen) and purification on RNeasy spin columns using RNeasy Minikit (Qiagen). Quantitative reverse transcription real-time PCR (qRT-PCR) was used to quantify the amounts of mRNA in the ears or lymph nodes using custom RT^2 Profiler PCR Arrays designed by us and manufactured by Qiagen/SA Biosciences, as previously described (19,20). The arrays typically included 30 to 54 assay genes, 5 housekeeping genes and reverse transcription efficiency and DNA contamination controls. All primer sets were from Qiagen/SA Biosciences, except the following primers designed by us: Pglyrp1, exons 1 and 2 primers, GTGGTGATCTCACACACAGC and GTGTGGTCACCCTTGATGTT; Pglyrp2, exons 3 and 4 primers, ACCAGGATGTGCGCAAGTGGGAT and AGTGACCCAGTGTAGTTGCCCA; and Pglyrp4, exons 4 and 5 primers, CGACCAGGGCTACAAGAA and CCAGGCAGTCTTCACTTTTC. cDNA was synthesized from 2 μg of RNA using RT^2 PCR Array First Strand Kit (Qiagen/SA Biosciences) and the arrays were performed according to the manufacturer instructions using Qiagen/SA Biosciences Master Mix. The lists of genes are provided in the figures. The experiments were performed on RNA pooled from 4–5 mice/group and repeated 3 times usually with another set of 4–5 mice/group (usually total of 8–10 mice per treatment).

For each gene, ΔCt was calculated using the same threshold (0.2) for all genes and Ct<35 considered as no expression, followed by normalization to 5 housekeeping genes (Hsp90ab1, Gusb, Hprt1, Gapdh, and Actb) included in each array, followed by calculation of ΔΔCt for each gene from two arrays: ΔΔCt = ΔCt1 – ΔCt2, where ΔCt1 is the TPA treated mice and ΔCT2 is the untreated mice, using the program provided by Qiagen/SA Biosciences. This calculation gives the fold increase in expression of each gene in the treated mice versus untreated mice per μg RNA and does not include in the calculation the increased amount of RNA obtained from the ears of TPA-treated mice compared to untreated mice (and thus the increases in gene expression would be greater if calculated per ear, rather than per μg RNA). The genomic DNA contamination controls, reverse

transcription controls, and positive PCR controls were included in each array and were all passed. Additional control to assure amplification from RNA, but not from possible contaminating DNA included parallel reaction sets from which reverse transcriptase was omitted, and which showed no amplification. To compare baseline gene expression in untreated mice, ΔCT1 was from untreated PGRP-deficient mice and ΔCT2 was from untreated WT mice.

The results were reported as mean fold increases after TPA treatment (treated/untreated) for WT mice, or ratios of fold increases in *Pglyrp*-deficient to WT mice, calculated as follows: [(*Pglyrp*$^{-/-}$ treated)/(*Pglyrp*$^{-/-}$ untreated)]/[(WT treated)/(WT untreated)] and presented as heat maps or bar graphs. The latter fold differences (ratios) of >1 or <1 reflect higher or lower expression levels of the genes (respectively) in *Pglyrp*-deficient than in WT mice. Heat maps were generated using Java TreeView after converting <1 ratios to negative fold difference using the formula: (−1)/ratio. The significance of differences in gene activation between groups of mice was determined using the two-sample one-tailed *t*-test, and typically the differences of >2 fold were significant at $P<0.05$.

Expression of mRNA for PGRPs was similarly measured by qRT-PCR using Qiagen/SA Biosciences First Strand Kit (with random primers) Qiagen/SA Biosciences SYBR Green Master Mix, and calculated using comparative cycle threshold method with 5 housekeeping genes (Hsp90ab1, Gusb, Hprt1, Gapdh, and Actb) as controls.

Isolation of cells and flow cytometry

Mouse ears were placed in RPMI-1640 with 3 mg/ml of Dispase II (Roche), separated into dorsal and ventral halves and scored on the dermal side with a scalpel. The tissue was digested for 8 hrs at 37°C in 5% CO_2. Dermis was then separated from the epidermis and epidermis was further digested with 0.25% trypsin in RPMI-1640 for 10 min at 37°C. Cells were washed 2x with RPMI-1640 with 5% fetal bovine serum (FBS) and incubated for 20 hrs in the same medium at 37°C in 5% CO_2. Cells were then strained through a 40 μm filter and resuspended at 2.0 x 10^7 cells/ml in RPMI-1640 with 5% FBS. Single cells from cervical lymph nodes and spleen were obtained by passing the tissue through a 40 μm filter, red blood cells were removed from the spleen cells with a lysis buffer (Biolegend), and cells were suspended at 2.0 x 10^7 cells/ml in RPMI-1640 with 5% FBS.

1 x10^6 cells were stained with CD4-APC (clone RM4-5, Biolegend) antibody for 20 min at 4°C. CD4-stained cells were then stained for Foxp3-PE (clone FJK-16s, eBioscience) or for cytokines IFN-γ-PE (clone XMG1.2), IL4-PE (clone 11B11) and IL-17-PE (clone TC11-18H10.1) with antibodies from Biolegend, used at 0.2 mg/1 x 10^6 cells according to Biolegend protocols using Biolegend buffers. Prior to staining for cytokines, CD4-APC stained cells were activated with TPA (25 ng/ml) and ionomycin (250 ng/ml) in the presence of the Golgi inhibitor, monensin, for 4 hrs at 37°C in 5% CO_2. Cells were analyzed by flow cytometry using MACSQuant (Miltenyi) cytometer. Foxp3, IFN-γ, IL-4 and IL-17 positive cells were measured within the $CD4^+$ gate (shown in the figures) and also within the entire lymphocyte gate (not shown).

Neutralization of IL-17, IL-22, and IL-1β

IL-17, IL-22, or IL-1β were neutralized by intravenous injections of endotoxin-free anti-IL-17 mAb (specific for IL-17A and not reactive with IL-1F, rat clone 50104, from R&D Systems), or anti-IL-22 mAb (rat clone IL22JOP from eBioscience), or anti-IL-1β (rat clone 30311 from R&D Systems), 100 μg on day 0 and 50 μg on days 3 and 6 of TPA treatment. These mAbs had equivalent neutralizing capacities for their respective cytokines based on the results provided by the manufacturers. Control mice were similarly treated with isotype

control rat IgG2aκ or IgG1 mAb (clone 16–4321 from eBioscience or clone 43414 from R&D Systems).

Results

Pglyrp2$^{-/-}$ mice have an enhanced inflammatory response to TPA in the skin

Repeated application of TPA (12-O-tetradecanoylphorbol 13-acetate) for 8 days (every other day) to the ears of WT BALB/c mice induced progressive moderate inflammation manifested by redness (Fig. 1A) and swelling (Fig. 1B). By contrast, similar application of TPA to *Pglyrp2*$^{-/-}$ mice induced significantly enhanced inflammation, manifested by increased redness (Fig. 1A) and significantly increased swelling, accompanied by severe scaling (Fig. 1A and B). This enhanced response was unique for *Pglyrp2*$^{-/-}$ mice, because it was not observed in *Pglyrp1*$^{-/-}$, *Pglyrp3*$^{-/-}$, and *Pglyrp4*$^{-/-}$ mice, and was dominant, because it was still observed in *Pglyrp1*$^{-/-}$*Pglyrp2*$^{-/-}$ and in *Pglyrp2*$^{-/-}$*Pglyrp3*$^{-/-}$ double-knockout mice (Fig. 1B). Deletion of *Pglyrp1* had an opposite effect on the early response to TPA, because *Pglyrp1*$^{-/-}$ single knockout, *Pglyrp1*$^{-/-}$*Pglyrp3*$^{-/-}$ double-knockout, and *Pglyrp1*$^{-/-}$*Pglyrp2*$^{-/-}$*Pglyrp3*$^{-/-}$ triple-knockout mice all showed reduced ear swelling on days 2 and 4 of TPA application, but not later (Fig. 1B). Deletion of *Pglyrp3* or *Pglyrp4* had little effect on the response to TPA. These results indicate that Pglyrp2 has a protective effect against severe TPA-induced psoriatic-like inflammation in WT mice, whereas Pglyrp1 has an enhancing proinflammatory effect in the early stages of the response.

We then compared the histology of TPA-induced skin lesions in WT and *Pglyrp*-deficient mice to determine the pathologic basis of this higher sensitivity of *Pglyrp2*$^{-/-}$ mice to TPA. Ears in untreated WT mice have one- to two-cell thick epidermis and few-cell thick subepidermal layer with blood vessels, sebaceous glands, hair follicles, muscle bundles, and central fat and connective tissue layer, with total thickness of approximately 200 μm. Histology of all untreated *Pglyrp*-deficient mice was similar to WT mice (Fig. 2A). Five TPA applications to the ears (every other day) induced strong inflammatory response that was very severe in *Pglyrp2*$^{-/-}$ mice. Cross-sections of the TPA-treated ears revealed severe acanthosis (thickening of the epidermis due to proliferation of keratinocytes), formation of rete pegs (downward papillary projections of epidermis), parakeratosis (retention of keratinocytes' nuclei in stratum corneum), parakeratotic scaling, formation of numerous epidermal microabscesses (primarily neutrophilic), and marked thickening of the sub-epidermal layer with dense cellular infiltrates (containing many PMNs and some mononuclear cells) that were all highly prominent in *Pglyrp2*$^{-/-}$ mice, *Pglyrp1*$^{-/-}$*Pglyrp2*$^{-/-}$mice (Fig. 2A) and all other double and triple knockout mice deficient in *Pglyrp2* (not shown). All these changes are highly characteristic of psoriatic lesions. WT mice (Fig. 2), *Pglyrp1*$^{-/-}$mice, *Pglyrp3*$^{-/-}$ mice, and *Pglyrp4*$^{-/-}$ mice (not shown) all showed significantly less severe acanthosis, rete pegs, parakeratosis, and parakeratotic scaling, less thickening of the subepidermal layer, and fewer cellular infiltrations, as judged by semi-quantitative evaluation of tissue sections (Fig. 2B). Measurements of the size of the microabscesses revealed significantly larger microabscesses in *Pglyrp2*$^{-/-}$ mice and *Pglyrp1*$^{-/-}$*Pglyrp2*$^{-/-}$ mice than in WT mice (Fig. 2B).

Our results demonstrate that deletion of *Pglyrp2*$^{-/-}$ highly predisposes mice to psoriatic-like lesions in response to TPA and the skin lesions in these mice have all main histological characteristics of human psoriatic lesions. Thus *Pglyrp2*$^{-/-}$ mice can serve as a convenient new mouse model of psoriasis-like inflammation. These results also further demonstrate that in WT mice Pglyrp2 protects the skin from excessive TPA-induced psoriasis-like inflammation.

Expression of PGRPs is increased in inflamed ears

We then compared expression of Pglyrp2 and other PGRPs in the ears in untreated and TPA-treated mice to gain further insight how Pglyrp2 influences sensitivity to TPA-induced inflammation. Treatment with TPA induced increased Pglyrp1 expression in the ears in all strains of mice (except *Pglyrp1*$^{-/-}$ mice) that was significantly higher than in untreated mice (Fig. 3). The expression of Pglyrp1 in the ears was significantly higher in all *Pglyrp2*$^{-/-}$mice^{-} than in WT mice at all time points following TPA treatment, which correlates with their higher inflammatory response and is likely due to increased infiltration with PMNs, which highly express Pglyrp1. The expression of Pglyrp2 in the ears significantly increased 6 hrs after the first TPA treatment and subsequently declined on days 3 through 9 (Fig. 3), which inversely correlates with the extent of inflammatory response and is consistent with the anti-inflammatory effect of Pglyrp2 in the TPA-induced inflammation model. Pglyrp3 has high constitutive expression in untreated skin. Following TPA treatment, Pglyrp3 expression initially increased in the ears and then declined. Pglyrp4 has much lower constitutive expression in untreated skin than Pglyrp3. Following TPA treatment, expression of Pglyrp4 was highly increased and was especially high in *Pglyrp2*$^{-/-}$*Pglyrp3*$^{-/-}$ mice (Fig. 3), indicating a compensatory expression of Pglyrp4 in mice deficient in *Pglyrp3*, since *Pglyrp3* and *Pglyrp4* genes are tightly linked in the psoriasis sensitivity locus on chromosome 3 in mice and their expression is correlated with the expression of keratinocytes differentiation genes (18). Thus, a decrease in Pglyrp3 expression is a consequence of the increased proliferation and de-differentiation of keratinocytes in the psoriasis model. These changes in Pglyrp3 and Pglyrp4 expression, however, had no detectable effect on the TPA-induced inflammation, which was similar in WT and *Pglyrp3*$^{-/-}$ and *Pglyrp4*$^{-/-}$ mice (Fig. 1B).

Pglyrp1 and Pglyrp2 were also constitutively expressed in the cervical lymph nodes at a similar level as in the ears, but following TPA treatment their expression in the cervical lymph nodes did not significantly change (data not shown). Pglyrp3 and Pglyrp4 were not constitutively expressed in cervical lymph nodes and their expression there was not induced following TPA treatment (data not shown). The above results indicate that the expression of Pglyrp1 and Pglyrp2 in the ear tissue cells but not in immune cells (cervical lymph nodes, which contain lymphocytes and antigen-presenting cells) correlates with the changes in inflammatory skin responses.

Pglyrp2$^{-/-}$ mice have increased Th17 cells and Th17 responses in the skin

We next studied the types of inflammatory cells in the ears in TPA-treated mice to determine the cellular basis for the differences in the inflammatory response in *Pglyrp2*$^{-/-}$ mice. We then determined which cell types significantly differed in *Pglyrp2*$^{-/-}$ mice compared to WT mice. This was first accomplished by measuring the amounts of mRNA for several marker genes characteristic of various immune and inflammatory cell types in the untreated and the affected ears. To determine which marker genes (and thus cell types) are increased or decreased in *Pglyrp2*$^{-/-}$ mice compared to WT mice, we calculated how many times higher or lower they were induced in *Pglyrp2*$^{-/-}$ mice than in WT mice (fold induction in *Pglyrp2*$^{-/-}$ mice/fold induction in WT mice).

Treatment with TPA for 9 days highly increased the numbers of monocytes and PMNs in the affected ears in WT mice (Fig. 4A, WT panel, and Supplemental Fig. 1). Keratinocyte differentiation marker, loricrin (Lor), was decreased, as was Ccr10 (the receptor for keratinocyte-specific chemokine, Ccl27), whereas antimicrobial peptides, β-defensin-3 (Defb3), calgranulin A (s100a8), and calgranulin B (s100a9) were greatly increased (Fig. 4A, WT panel, and Supplemental Fig. 1), reflecting de-differentiated and activated state of keratinocytes, consistent with TPA-induced proliferation of keratinocytes. These are all

expected changes consistent with the psoriasis model. *Pglyrp*-deficient mice that had enhanced response to TPA (*Pglyrp2*$^{-/-}$, *Pglyrp1*$^{-/-}$*Pglyrp2*$^{-/-}$, and *Pglyrp2*$^{-/-}$*Pglyrp3*$^{-/-}$ mice) had significantly higher increases in PMNs and monocytes compared to WT mice, as well as increased B cells and T cells, and especially Rorγt-expressing cells (Fig. 4A, *Pglyrp*$^{-/-}$/WT panel, and Supplemental Fig. 1), which are characteristically (but not exclusively) Th17 cells (24). These results suggest that the common cell type preferentially increased in *Pglyrp*-deficient mice that are more sensitive to TPA-induced psoriasis-like inflammation compared to WT mice may be the Rorγt-expressing Th17 cells.

We then measured the expression of an extended panel of cytokines, chemokines, and other marker genes characteristic of Th1, Th2, Th17, Treg, NK, and other cell types to further define the cell types responsible for the increased sensitivity of *Pglyrp2*$^{-/-}$ mice to TPA-induced skin inflammation, and to determine which of these genes were differentially induced in the affected skin in *Pglyrp*-deficient mice, compared to WT mice. We included these cell types, because in addition to Th1 and Th2 cells, Th17 cells and other cell types may also be involved in skin inflammation.

TPA is a diacylglycerol analog that activates many immune and non-immune cell types through the activation of protein kinase C. In our model, a single exposure to TPA highly activated multiple genes in many cell types in WT mice – 6 hrs after a single TPA treatment 17 out of 49 genes were induced more than 15-fold (Fig. 4B, WT 6 hrs panel, and Supplemental Fig. 2). In *Pglyrp2*$^{-/-}$, *Pglyrp1*$^{-/-}$*Pglyrp2*$^{-/-}$, and *Pglyrp2*$^{-/-}$*Pglyrp3*$^{-/-}$ mice a single exposure to TPA in 6 hrs induced moderately higher activation of genes characteristic of Th17 cells and some genes characteristic of multiple cell types (Fig. 4B, *Pglyrp*$^{-/-}$/WT 6 hrs panel, and Supplemental Fig. 2). TPA treatment for 9 days induced prolonged inflammation in all mice, but WT mice were able to reduce the number of highly activated (more than 15-fold) genes to only five genes, namely Cxcl2 and Cxcl5 (characteristic of Th17 cells), and Ccl3, Ccl4, and Il1b (characteristic of multiple cell types) (Fig. 4B, WT 9 days panel, and Supplemental Fig. 3), compared to 17 genes highly induced 6 hrs after the first TPA treatment. By contrast, *Pglyrp2*$^{-/-}$, *Pglyrp1*$^{-/-}$*Pglyrp2*$^{-/-}$, and *Pglyrp2*$^{-/-}$*Pglyrp3*$^{-/-}$ mice, which showed increased clinical responses to TPA (Figs 1 and 2), were not able to reduce the number of TPA-activated genes after 9 days of TPA treatment, and had many genes induced several fold higher than WT mice – six genes characteristic of Th17 cells and eight genes characteristic of other cell types were induced more than three-fold higher in *Pglyrp2*$^{-/-}$, *Pglyrp1*$^{-/-}$*Pglyrp2*$^{-/-}$, and *Pglyrp2*$^{-/-}$*Pglyrp3*$^{-/-}$ mice than in WT mice (Fig. 4B, *Pglyrp*$^{-/-}$/WT 9 days panel, and Supplemental Fig. 3).

The above results indicate that the *Pglyrp2*$^{-/-}$ mice that have higher skin responsiveness to TPA have increased activity of Th17 cells in the affected skin, compared to WT mice. We then used flow cytometry to directly measure Th cell types in the ears, draining lymph nodes, and the spleen, to further investigate the role of Th17 cells (and other Th cell types) in increased sensitivity of *Pglyrp*-deficient mice to TPA-induced psoriasis-like skin inflammation (Fig. 5A and B).

TPA treatment for 9 days induced a substantial accumulation of CD4$^+$ cells in the TPA-treated skin. Untreated ears in WT and *Pglyrp2*$^{-/-}$ mice had ~400 CD4$^+$ cells/ear, whereas on day 9 after five TPA treatments the numbers of CD4$^+$ cells/ear increased to ~15,000/ear in WT mice and ~27,000/ear in *Pglyrp2*$^{-/-}$ mice, which is significantly higher than in WT mice (Fig. 5B). A moderate increase in the amount of CD4 mRNA detected by qRT-PCR (Fig. 4A and Supplemental Fig. 1) is an underestimation due to undetectable amount of CD4 mRNA in the untreated ears.

Th17 cells ($CD4^+IL\text{-}17^+$) were undetectable in the ears of untreated mice (<10 Th17 cells/ear, not shown). TPA treatment for 9 days induced accumulation of Th17 cells in the ears and their percentages were significantly higher in the affected ears in *Pglyrp2*$^{-/-}$ and *Pglyrp1*$^{-/-}$*Pglyrp2*$^{-/-}$ mice compared to WT mice (Fig. 5A). If the numbers of Th17 cells are calculated based on the total numbers of $CD4^+$ cells in the TPA-treated ears (Fig. 5B), the total numbers of Th17 cells increased from <10 Th17 cells/ear in untreated mice to ~375 Th17 cells/ear in WT mice and >1,600 Th17 cells/ear in *Pglyrp1*$^{-/-}$*Pglyrp2*$^{-/-}$ mice (which is >4 times more Th17 cells/ear in *Pglyrp1*$^{-/-}$*Pglyrp2*$^{-/-}$ mice than in WT mice). By contrast, there was no significant difference in the percentages of Th1 ($CD4^+IFN\text{-}\gamma^+$) and Th2 ($CD4^+IL\text{-}4^+$) cells in the ears of WT and *Pglyrp2*$^{-/-}$ and *Pglyrp1*$^{-/-}$*Pglyrp2*$^{-/-}$ mice (Fig. 5A). Virtually all detectable $IL\text{-}17^+$ cells in the TPA-treated ears were $CD4^+$ (Th17 cells) and there were very few (<50/ear, not shown) other $IL\text{-}17^+$ cells in the inflamed skin (such as $CD8^+$, γ/δ T cells, or NKT cells), and therefore the observed increases in $IL\text{-}17^+$ cells mostly represent increases in Th17 cells ($CD4^+IL\text{-}17^+$).

TPA-treated mice had substantially swollen cervical lymph nodes (>3 mm in diameter, compared to <0.5 mm in untreated mice) and the numbers of all Th cell types were significantly higher in *Pglyrp2*$^{-/-}$ and *Pglyrp1*$^{-/-}$*Pglyrp2*$^{-/-}$ mice compared to WT mice in the cervical lymph nodes, and to lesser extent in the spleen (Fig. 5A). These results indicate preferential recruitment and retention of Th17 cells in the TPA-treated ears in *Pglyrp2*$^{-/-}$ and *Pglyrp1*$^{-/-}$*Pglyrp2*$^{-/-}$ mice compared to WT mice, consistent with our mRNA gene expression data.

IL-17 is required for enhanced response to TPA in *Pglyrp2*$^{-/-}$ mice

We then compared the severity of ear inflammation in TPA-treated *Pglyrp1*$^{-/-}$*Pglyrp2*$^{-/-}$mice in which IL-17 activity was inhibited with neutralizing anti-IL-17 mAb to determine whether IL-17 (Th17 cytokine) is required in vivo for the high sensitivity of *Pglyrp2*$^{-/-}$ mice to TPA-induced psoriasis-like inflammation. In vivo neutralization of IL-17 activity in *Pglyrp1*$^{-/-}$*Pglyrp2*$^{-/-}$ mice significantly decreased TPA-induced ear inflammation, compared to mice treated with an isotype control IgG (Fig. 5C), reducing it back to the level of inflammation seen in WT mice (compare 35–40% decrease in ear swelling in *Pglyrp1*$^{-/-}$*Pglyrp2*$^{-/-}$ mice treated with anti-IL-17 mAb relative to isotype control IgG in Fig. 5C, to 35–40% increase in ear swelling in *Pglyrp1*$^{-/-}$*Pglyrp2*$^{-/-}$ mice relative to WT mice in Fig. 1B).

One of the main Th17 cell effector cytokines induced by IL-17 is IL-22 (which in turn induces production of PMN-attracting chemokines in keratinocytes). We thus also evaluated the in vivo role of IL-22 in the TPA-induced skin inflammation, because PMNs were the most prominent infiltrating inflammatory cells in this model. Treatment of *Pglyrp1*$^{-/-}$*Pglyrp2*$^{-/-}$ mice with neutralizing anti-IL-22 mAbs significantly reduced ear inflammation in this model, compared to mice treated with an isotype control IgG (Fig. 5C), causing ~75% reversal of enhanced swelling in *Pglyrp1*$^{-/-}$*Pglyrp2*$^{-/-}$ mice relative to WT mice (compare differences in swelling in Fig. 5C to Fig. 1B). These results show that IL-22 is one of the main IL-17-induced cytokines, but not the only one, responsible for the higher skin inflammatory responsiveness of *Pglyrp2*$^{-/-}$ mice compared to WT mice.

Our results demonstrate that IL-17 and IL-22 are required for manifestation of the enhanced skin inflammation in *Pglyrp2*$^{-/-}$ mice in the TPA-induced psoriasis-like inflammation model.

Pglyrp2$^{-/-}$ mice have decreased numbers of Treg cells in the skin

We then tested whether the ability of WT mice to limit TPA-induced skin inflammation more effectively than *Pglyrp2*$^{-/-}$ mice is due to impaired generation or function of regulatory T cells ($CD4^+FoxP3^+$ Treg) in *Pglyrp2*$^{-/-}$ mice. TPA-treated WT mice very efficiently recruited Treg cells into the affected skin, as evidenced by an increase in FoxP3-expressing cells in the affected skin shown both by the qRT-PCR (Fig. 4) and by flow cytometry, which revealed high numbers of $CD4^+FoxP3^+$ cells in the affected skin in WT mice (Fig. 5A). By contrast, *Pglyrp*-deficient mice that had enhanced inflammatory responses (*Pglyrp2*$^{-/-}$, *Pglyrp1*$^{-/-}$*Pglyrp2*$^{-/-}$ and *Pglyrp2*$^{-/-}$*Pglyrp3*$^{-/-}$ mice) all had lower expression of FoxP3 mRNA in the affected ears compared to WT mice (Fig. 4A and Supplemental Fig. 1). TPA-treated *Pglyrp2*$^{-/-}$ and *Pglyrp1*$^{-/-}$*Pglyrp2*$^{-/-}$ mice also had significantly lower numbers of $CD4^+FoxP3^+$ Treg cells in the affected skin compared to WT mice measured by flow cytometry (Fig. 5A). These results suggest impaired recruitment and/or maintenance of Treg cells in the inflamed skin in *Pglyrp2*$^{-/-}$ mice.

We also compared the numbers of Treg cells in the draining cervical lymph nodes and in the spleen of TPA-treated WT and *Pglyrp2*$^{-/-}$ mice to further investigate whether *Pglyrp2*$^{-/-}$ mice have less efficient generation of induced Treg cells in lymphoid tissues in general or less efficient recruitment and/or maintenance of these cells in the inflamed skin. *Pglyrp2*$^{-/-}$ and *Pglyrp1*$^{-/-}$*Pglyrp2*$^{-/-}$ mice treated with TPA had significantly higher numbers of Treg cells in the cervical lymph nodes and in the spleen than TPA-treated WT mice (Fig. 5A). These results indicate that *Pglyrp2*$^{-/-}$ and *Pglyrp1*$^{-/-}$*Pglyrp2*$^{-/-}$ mice are able to generate induced Treg cells in lymphoid organs, and suggest that they are less efficient than WT mice in recruiting these cells to the inflamed skin and/or retaining them in the skin.

There could be at least two reasons for this less efficient recruitment of Treg cells to the skin in *Pglyrp2*$^{-/-}$ mice: insufficient production of Treg-attracting chemokines in the skin, and/or insufficient expression of receptors for these chemokines in Treg cells in *Pglyrp2*$^{-/-}$ mice. Our results show lower levels of mRNA for Treg-attracting chemokines (Ccl1, Ccl17, and Ccl27a) in *Pglyrp2*$^{-/-}$ mice compared to WT mice (Fig. 4B, *Pglyrp*$^{-/-}$/WT 9 days panel, and Supplemental Fig. 3), indicating insufficient production of Treg-attracting chemokines in the skin in *Pglyrp2*$^{-/-}$mice. To investigate the second of the above-mentioned possibilities, we determined whether Treg cells in the draining cervical lymph nodes in *Pglyrp2*$^{-/-}$ mice had sufficient expression of receptors for Treg-attracting chemokines (Ccr4, Ccr8, and Ccr10). Treatment of the ears with TPA for 9 days induced significantly higher levels of mRNA for Ccr4, Ccr8, and Ccr10 in the draining cervical lymph nodes in *Pglyrp1*$^{-/-}$*Pglyrp2*$^{-/-}$ mice compared to WT mice (Fig. 5D), consistent with higher numbers of Treg cells in the cervical lymph nodes of *Pglyrp1*$^{-/-}$*Pglyrp2*$^{-/-}$mice compared to WT mice (Fig. 5A). These results indicate that Treg cells in the draining lymph nodes in TPA-treated *Pglyrp2*$^{-/-}$ mice have sufficient expression of receptors for Treg-attracting chemokines, but that these cells are not recruited to the inflamed skin, likely because of the insufficient production of Treg-attracting chemokines in the skin, as shown above (Fig. 4B and Supplemental Fig. 3). Our results thus indicate that in WT mice Pglyrp2 promotes efficient population of the skin with Treg cells in the TPA-induced psoriasis-like inflammation.

IL-1β is not responsible for the enhanced response to TPA in *Pglyrp2*$^{-/-}$ mice

IL-1β is an important pro-inflammatory cytokine produced by many cell types, and in our model of TPA-induced ear inflammation IL-1β mRNA was highly induced by TPA in WT mice and it was also induced higher in the TPA-sensitive *Pglyrp2*$^{-/-}$ mice than in WT mice (Fig. 4B and Supplemental Fig. 3). To determine whether IL-1β is required in vivo for the high sensitivity of *Pglyrp2*$^{-/-}$ mice to TPA-induced skin inflammation, we determined the

severity of ear inflammation in TPA-treated *Pglyrp1*$^{-/-}$*Pglyrp2*$^{-/-}$ mice in which IL-1β activity was inhibited with neutralizing anti-IL-1β mAb. In vivo neutralization of IL-1β activity in *Pglyrp1*$^{-/-}$*Pglyrp2*$^{-/-}$ mice had no effect on TPA-induced ear inflammation, compared to mice treated with an isotype control IgG (Fig. 6A). Both groups of mice (anti-IL-1β mAb and control IgG-treated *Pglyrp1*$^{-/-}$*Pglyrp2*$^{-/-}$ mice) also had similar numbers of Th17 and Treg cells in TPA-treated skin (Fig. 6B and C). These results indicate that IL-1β is not responsible for the increased inflammatory response to TPA in *Pglyrp2*$^{-/-}$ mice and for the decreased numbers of Treg cells and increased numbers of Th17 cells in the skin of these mice following TPA treatment, and, thus, increased IL-1β production in TPA-treated *Pglyrp2*$^{-/-}$ mice is a consequence, but not the cause of increased skin inflammation in *Pglyrp2*$^{-/-}$ mice.

Discussion

We demonstrate that *Pglyrp2*$^{-/-}$ mice develop more severe TPA-induced psoriasis-like inflammation than WT mice. Thus, in WT mice, Pglyrp2 protects mice from the development of TPA-induced psoriasis-like inflammation. The mechanism underlying increased sensitivity of *Pglyrp2*$^{-/-}$ mice to TPA-induced inflammation is decreased recruitment and activity of Treg cells and enhanced production and activation of Th17 cells in the affected skin, which results in more severe inflammation and keratinocyte proliferation. Thus, in WT mice, Pglyrp2 promotes recruitment and retention of Treg cells in the inflamed skin, which limits over-activation of Th17 cells and protects the skin from exaggerated inflammatory response.

Th17 cells were originally thought to play a role in some autoimmune diseases and in recruitment of PMNs to the sites of inflammation (25–28), but they have many other functions. They play a role in inflammatory bowel diseases, skin diseases, asthma, graft rejection, atherosclerosis, periodontal disease, and arthritis (29–31). We extend these findings by showing that Th17 cells exacerbate skin inflammation in the experimental model of TPA-induced psoriasis-like inflammation in a Pglyrp2-dependent manner. Psoriasis was originally thought to have Th1 bias, but it involves complex interactions of many cell types and lately is considered to have Th17 bias (2,32–37). Our results support this view and indicate that Pglyrp2 is involved in the control of Th17 cells in the inflamed skin, because increased Th17 activity and their increased recruitment to the skin are associated with more severe psoriasis-like inflammatory phenotype in *Pglyrp2*$^{-/-}$ mice.

Our results show that Pglyrp2, a member of a family of innate immunity proteins, affects the functions of both innate and adaptive immune cells with an outcome of enhancing the recruitment and activity of Treg cells and inhibiting the activity of Th17 cells. *Pglyrp2*$^{-/-}$mice have decreased numbers of Treg cells and increased numbers of Th17 cells in the inflamed skin, compared to WT mice. Proinflammatory stimuli (such as TPA) in WT mice initially induce vigorous cytokine and chemokine production. However, upon chronic exposure, WT mice are able to recruit and maintain large numbers of Treg cells in the inflamed skin and are able to limit the proinflammatory response by both drastically reducing the number of proinflammatory genes that are activated and reducing the level of their activation. By contrast, *Pglyrp2*$^{-/-}$ mice have fewer Treg cells and higher numbers of Th17 cells in the affected skin and are unable to limit inflammatory responses.

Human skin is also enriched in Treg cells compared to peripheral blood and lymphoid organs – up to 80% of CD4$^+$ T cells could be Foxp3$^+$ Treg cells in the skin of healthy control individuals (38). In contrast to these healthy controls, patients with psoriasis (similar to *Pglyrp2*$^{-/-}$ mice with psoriasis-like skin inflammation) have lower percentages of Treg cells in the affected skin, for example 33% (38), 45% (39), or 50% (40) of total CD4$^+$ cells.

Thus, deficient recruitment, generation, or maintenance of Treg cells also seems to be a feature of human psoriasis and may be a significant factor contributing to the sensitivity to psoriasis in humans, although this aspect has not been sufficiently studied in human psoriasis.

There may be multiple reasons for the imbalance in Treg/Th17 cells that we observed in *Pglyrp2*$^{-/-}$ mice. It could come from reduced recruitment of Treg cells and increased recruitment of Th17 cells to the affected skin, and/or from enhanced local differentiation of T cells into Th17 cells (including conversion of Treg cells into Th17 cells) under the influence of locally-produced chemokines and cytokines. T cell populations are dynamic and have considerable plasticity based on local cytokine milieu, as, for example, Treg cells can differentiate into Th17 cells under the influence of locally-produced proinflammatory cytokines (41,42). The enhanced recruitment and differentiation of Th17 cells is supported by higher production of Th17 cell promoting cytokines (IL-17, IL-22, IL-23) in the inflamed skin in *Pglyrp2*$^{-/-}$ mice. Decreased recruitment of Treg cells to the inflamed skin is supported by the presence of higher numbers of Treg cells in the draining lymph nodes and spleen in TPA-treated *Pglyrp2*$^{-/-}$ mice than in WT mice, but lower numbers in the skin. These Treg cells in the draining lymph nodes in *Pglyrp2*$^{-/-}$ mice express receptors for Treg-attracting chemokines (CCR4, CCR8, and CCR10), yet do not migrate in sufficient numbers to the inflamed skin. These results suggest efficient generation of induced Treg cells in lymphoid organs but defective recruitment to the inflamed skin. This mechanism is further supported by decreased production of Treg cell-attracting chemokines (CCL1, CCL17, CCL27) in the skin of *Pglyrp2*$^{-/-}$ mice. Thus both increased recruitment and generation of Th17 cells and decreased recruitment and retention of Treg cells in the skin are likely responsible for increased inflammation in *Pglyrp2*$^{-/-}$ mice.

Pglyrp2 is primarily expressed in the liver and its expression is induced in other non-immune cells, including keratinocytes (4,5,15,17). Keratinocytes are an important local source of chemokines and cytokines, and activation of keratinocytes by proinflammatory stimuli and increased expression of Pglyrp2 correlates with the ability of WT mice to reduce chronic inflammation in the skin. The lack of Pglyrp2 correlates with increased inflammation in *Pglyrp2*$^{-/-}$ mice. The effects of Pglyrp2 in the inflamed skin are likely exerted through a change in the local production of chemokines and cytokines in the skin, which modulates the recruitment and activity of these Treg and Th17 cells. Thus, in *Pglyrp2*$^{-/-}$ mice reduced numbers of Treg cells allow dominating expansion of Th17 cells, which can increase inflammatory responses in the skin. Therefore, in WT mice compared to *Pglyrp2*$^{-/-}$ mice, the immune balance is shifted towards Treg cells that control detrimental inflammation induced by proinflammatory Th17 cells. Our results suggest that defects in the *Pglyrp2* gene could be predisposing to psoriasis-like skin inflammation through the aforementioned shift in immune homeostasis.

Supplementary Material

Refer to Web version on PubMed Central for supplementary material.

Acknowledgments

We are grateful to Patrick Bankston for help in interpreting histology slides, and Robert Rukavina, Julie Cook, Panida Girddonfag, and Tiffany Caluag for maintaining and breeding our mice.

Abbreviations

PGRP or Pglyrp	peptidoglycan recognition protein

TPA	12-O-tetradecanoylphorbol 13-acetate

References

1. Mrowietz U, Elder JT, Barker J. The importance of disease associations and concomitant therapy for the long-term management of psoriasis patients. Arch Dermatol Res. 2006; 298:309–319. [PubMed: 17021761]
2. Elder JT, Bruce AT, Gudjonsson JE, Johnston A, Stuart PE, Tejasvi T, Voorhees JJ, Abecasis GR, Nair RP. Molecular dissection of psoriasis: integrating genetics and biology. J Invest Dermatol. 2010; 130:1213–1226. [PubMed: 19812592]
3. Kang D, Liu G, Lundstrom A, Gelius E, Steiner H. A peptidoglycan recognition protein in innate immunity conserved from insects to humans. Proc Natl Acad Sci USA. 1998; 95:10078–10082. [PubMed: 9707603]
4. Liu C, Xu Z, Gupta D, Dziarski R. Peptidoglycan recognition proteins: a novel family of four human innate immunity pattern recognition molecules. J Biol Chem. 2001; 276:34686–34694. [PubMed: 11461926]
5. Lu X, Wang M, Qi J, Wang H, Li X, Gupta D, Dziarski R. Peptidoglycan recognition proteins are a new class of human bactericidal proteins. J Biol Chem. 2006; 281:5895–5907. [PubMed: 16354652]
6. Tydell CC, Yuan J, Tran P, Selsted ME. Bovine peptidoglycan recognition protein-S: antimicrobial activity, localization, secretion, and binding properties. J Immunol. 2006; 176:1154–1162. [PubMed: 16394004]
7. Wang M, Liu LH, Wang S, Li X, Lu X, Gupta D, Dziarski R. Human peptidoglycan recognition proteins require zinc to kill both Gram-positive and Gram-negative bacteria and are synergistic with antibacterial peptides. J Immunol. 2007; 178:3116–3125. [PubMed: 17312159]
8. Kashyap DR, Wang M, Liu LH, Boons GJ, Gupta D, Dziarski R. Peptidoglycan recognition proteins kill bacteria by activating protein-sensing two-component systems. Nature Med. 2011; 17:676–683. [PubMed: 21602801]
9. Gelius E, Persson C, Karlsson J, Steiner H. A mammalian peptidoglycan recognition protein with N-acetylmuramoyl-L-alanine amidase activity. Biochem Biophys Res Commun. 2003; 306:988–994. [PubMed: 12821140]
10. Wang ZM, Li X, Cocklin RR, Wang M, Wang M, Fukase K, Inamura S, Kusumoto S, Gupta D, Dziarski R. Human peptidoglycan recognition protein-L is an N-acetylmuramoyl-L-alanine amidase. J Biol Chem. 2003; 278:49044–49052. [PubMed: 14506276]
11. Liu C, Gelius E, Liu G, Steiner H, Dziarski R. Mammalian peptidoglycan recognition protein binds peptidoglycan with high affinity, is expressed in neutrophils, and inhibits bacterial growth. J Biol Chem. 2000; 275:24490–24499. [PubMed: 10827080]
12. Dziarski R, Platt KA, Gelius E, Steiner H, Gupta D. Defect in neutrophil killing and increased susceptibility to infection with non-pathogenic Gram-positive bacteria in peptidoglycan recognition protein-S (PGRP-S)-deficient mice. Blood. 2003; 102:689–697. [PubMed: 12649138]
13. Lo D, Tynan W, Dickerson J, Mendy J, Chang HW, Scharf M, Byrne D, Brayden D, Higgins L, Evans C, O'Mahony DJ. Peptidoglycan recognition protein expression in mouse Peyer's Patch follicle associated epithelium suggests functional specialization. Cell Immunol. 2003; 224:8–16. [PubMed: 14572796]
14. Xu M, Wang Z, Locksley RM. Innate immune responses in peptidoglycan recognition protein L-deficient mice. Mol Cell Biol. 2004; 24:7949–7957. [PubMed: 15340057]
15. Wang H, Gupta D, Li X, Dziarski R. Peptidoglycan recognition protein 2 (N-acetylmuramoyl-L-Ala amidase) is induced in keratinocytes by bacteria through the p38 kinase pathway. Infect Immun. 2005; 73:7216–7225. [PubMed: 16239516]
16. Zhang Y, van der Fits L, Voerman JS, Melief M-JJD, Laman, Wang M, Wang H, Wang M, Li X, Walls CD, Gupta D, Dziarski R. Identification of serum *N*-acetylmuramoyl-L-alanine amidase as liver peptidoglycan recognition protein 2. Biochim Biophys Acta. 2005; 1752:34–46. [PubMed: 16054449]

17. Li X, Wang S, Wang H, Gupta D. Differential expression of peptidoglycan recognition protein 2 in the skin and liver requires different transcription factors. J Biol Chem. 2006; 281:20738–20748. [PubMed: 16714290]
18. Mathur P, Murray B, Crowell T, Gardner H, Allaire N, Hsu YM, Thill G, Carulli JP. Murine peptidoglycan recognition proteins PglyrpIα and PglyrpIβ are encoded in the epidermal differentiation complex and are expressed in epidermal and hematopoietic tissues. Genomics. 2004; 83:1151–1163. [PubMed: 15177568]
19. Saha S, Jing X, Park SY, Wang S, Li X, Gupta D, Dziarski R. Peptidoglycan Recognition Proteins protect mice from experimental colitis by promoting normal gut flora and preventing induction of interferon-γ. Cell Host Microbe. 2010; 8:147–162. [PubMed: 20709292]
20. Saha S, Qi J, Wang S, Wang M, Li X, Kim Y-G, Núñez G, Gupta D, Dziarski R. PGLYRP-2 and Nod2 are both required for peptidoglycan-induced arthritis and local inflammation. Cell Host Microbe. 2009; 5:137–150. [PubMed: 19218085]
21. Sun C, Mathur P, Dupuis J, Tizard R, Ticho B, Crowell T, Gardner H, Bowcock AM, Carulli J. Peptidoglycan recognition proteins Pglyrp3 and Pglyrp4 are encoded from the epidermal differentiation complex and are candidate genes for the Psors4 locus on chromosome 1q21. Hum Genet. 2006; 119:113–125. [PubMed: 16362825]
22. Kainu K, Kivinen K, Zucchelli M, Suomela S, Kere J, Inerot A, Baker BS, Powles AV, Fry L, Samuelsson L, Saarialho-Kere U. Association of psoriasis to PGLYRP and SPRR genes at PSORS4 locus on 1q shows heterogeneity between Finnish, Swedish and Irish families. Exp Dermatol. 2009; 18:109–115. [PubMed: 18643845]
23. Hvid H, Teige I, Kvist PH, Svensson L, Kemp K. TPA induction leads to a Th17-like response in transgenic K14/VEGF mice: a novel in vivo screening model of psoriasis. Int Immunol. 2008; 20:1097–1106. [PubMed: 18579711]
24. Ivanov II, McKenzie BS, Zhou L, Tadokoro CE, Lepelley A, Lafaille JJ, Cua DJ, Littman DR. The orphan nuclear receptor RORγt directs the differentiation program of proinflammatory IL-17^{+} T helper cells. Cell. 2006; 126:1121–1133. [PubMed: 16990136]
25. Ye P, Rodriguez FH, Kanaly S, Stocking KL, Schurr J, Schwarzenberger P, Oliver P, Huang W, Zhang P, Zhang J, Shellito JE, Bagby GJ, Nelson S, Charrier K, Peschon JJ, Kolls JK. Requirement of interleukin 17 receptor signaling for lung CXC chemokine and granulocyte colony-stimulating factor expression, neutrophil recruitment, and host defense. J Exp Med. 2001; 194:519–527. [PubMed: 11514607]
26. Cua DJ, Sherlock J, Chen Y, Murphy CA, Joyce B, Seymour B, Lucian L, To W, Kwan S, Churakova T, Zurawski S, Wiekowski M, Lira SA, Gorman D, Kastelein RA, Sedgwick JD. Interleukin-23 rather than interleukin-12 is the critical cytokine for autoimmune inflammation of the brain. Nature. 2003; 421:744–748. [PubMed: 12610626]
27. Murphy CA, Langrish CL, Chen Y, Blumenschein W, McClanahan T, Kastelein RA, Sedgwick JD, Cua DJ. Divergent pro- and antiinflammatory roles for IL-23 and IL-12 in joint autoimmune inflammation. J Exp Med. 2003; 198:1951–1957. [PubMed: 14662908]
28. Langrish CL, Chen Y, Blumenschein WM, Mattson J, Basham B, Sedgwick JD, McClanahan T, Kastelein RA, Cua DJ. IL-23 drives a pathogenic T cell population that induces autoimmune inflammation. J Exp Med. 2005; 201:233–240. [PubMed: 15657292]
29. Korn T, Bettelli E, Oukka M, Kuchroo VK. IL-17 and Th17 cells. Annu Rev Immunol. 2009; 27:485–517. [PubMed: 19132915]
30. Miossec P, Korn T, Kuchroo VK. Interleukin-17 and type 17 helper T cells. N Engl J Med. 2009; 361:888–898. [PubMed: 19710487]
31. Alcorn JF, Crowe CR, Kolls JK. TH17 cells in asthma and COPD. Annu Rev Physiol. 2010; 72:495–516. [PubMed: 20148686]
32. Zheng Y, Danilenko DM, Valdez P, Kasman I, Eastham-Anderson J, Wu J, Ouyang W. Interleukin-22, a T_H17 cytokine, mediates IL-23-induced dermal inflammation and acanthosis. Nature. 2007; 445:648–651. [PubMed: 17187052]
33. Ma HL, Liang S, Li J, Napierata L, Brown T, Benoit S, Senices M, Gill D, Dunussi-Joannopoulos K, Collins M, Nickerson-Nutter C, Fouser LA, Young DA. IL-22 is required for Th17 cell-

mediated pathology in a mouse model of psoriasis-like skin inflammation. J Clin Invest. 2008; 118:597–607. [PubMed: 18202747]

34. Blauvelt A. T-helper 17 cells in psoriatic plaques and additional genetic links between IL-23 and psoriasis. J Invest Dermatol. 2008; 128:1064–1067. [PubMed: 18408745]
35. Harper EG, Guo C, Rizzo H, Lillis JV, Kurtz SE, Skorcheva I, Purdy D, Fitch E, Iordanov M, Blauvelt A. Th17 cytokines stimulate CCL20 expression in keratinocytes in vitro and in vivo: implications for psoriasis pathogenesis. J Invest Dermatol. 2009; 129:2175–2183. [PubMed: 19295614]
36. van der Fits L, Mourits S, Voerman JS, Kant M, Boon L, Laman JD, Cornelissen F, Mus AM, Florencia E, Prens EP, Lubberts E. Imiquimod-induced psoriasis-like skin inflammation in mice is mediated via the IL-23/IL-17 axis. J Immunol. 2009; 182:5836–5845. [PubMed: 19380832]
37. Kagami S, Rizzo HL, Lee JJ, Koguchi Y, Blauvelt A. Circulating Th17, Th22, and Th1 cells are increased in psoriasis. J Invest Dermatol. 2010; 130:1373–1383. [PubMed: 20032993]
38. Antiga E, Quaglino P, Bellandi S, Volpi W, Del Bianco E, Comessatti A, Osella-Abate S, De Simone C, Marzano A, Bernengo MG, Fabbri P, Caproni M. Regulatory T cells in the skin lesions and blood of patients with systemic sclerosis and morphoea. Br J Dermatol. 2010; 162:1056–1063. [PubMed: 20105169]
39. Franz B, Fritzsching B, Riehl A, Oberle N, Klemke CD, Sykora J, Quick S, Stumpf C, Hartmann M, Enk A, Ruzicka T, Krammer PH, Suri-Payer E, Kuhn A. Low number of regulatory T cells in skin lesions of patients with cutaneous lupus erythematosus. Arthritis Rheum. 2007; 56:1910–1920. [PubMed: 17530636]
40. Fujimura T, Okuyama R, Ito Y, Aiba S. Profiles of Foxp3+ regulatory T cells in eczematous dermatitis, psoriasis vulgaris and mycosis fungoides. Br J Dermatol. 2008; 158:1256–1263. [PubMed: 18363755]
41. Zhou L, Chong MM, Littman DR. Plasticity of $CD4^+$ T cell lineage differentiation. Immunity. 2009; 30:646–655. [PubMed: 19464987]
42. Campbell DJ, Koch MA. Phenotypical and functional specialization of $FOXP3^+$ regulatory T cells. Nat Rev Immunol. 2011; 11:119–130. [PubMed: 21267013]

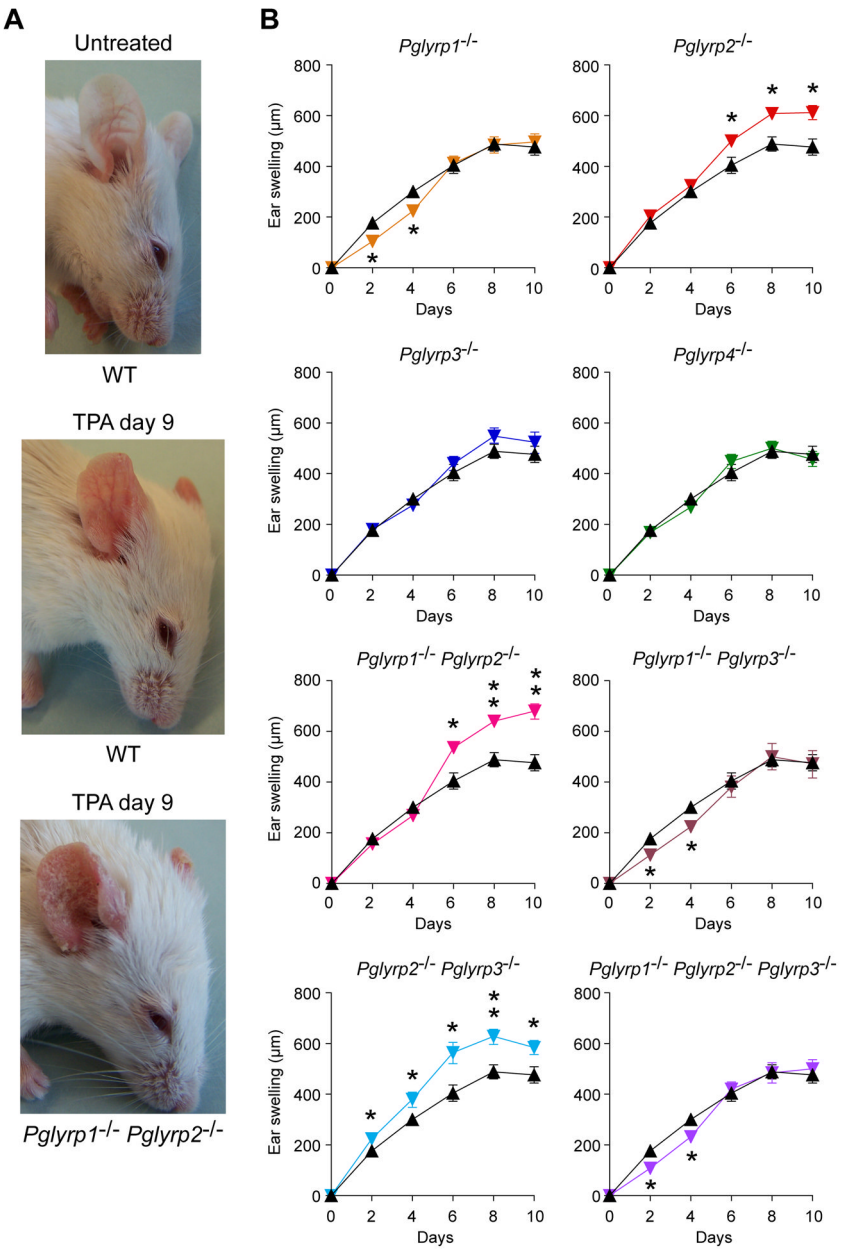

Figure 1. *Pglyrp2*$^{-/-}$ mice have enhanced response to TPA in the skin

(**A**) Application of TPA to ears for 9 days (every other day) induces mild inflammation in WT mice and severe inflammation in *Pglyrp1*$^{-/-}$*Pglyrp2*$^{-/-}$ mice with increased redness, swelling, and extensive scaling. (**B**) Ear swelling in WT mice (black triangles) and *Pglyrp*$^{-/-}$ mice (color triangles) after TPA application to the ears on days 0, 2, 4, 6, and 8; means ± SEM (SEM were often smaller than the symbols in this and other figures); N = 9–14 mice/group; significance of differences between *Pglyrp*$^{-/-}$ and WT mice: *, P<0.02; **, P<0.0001.

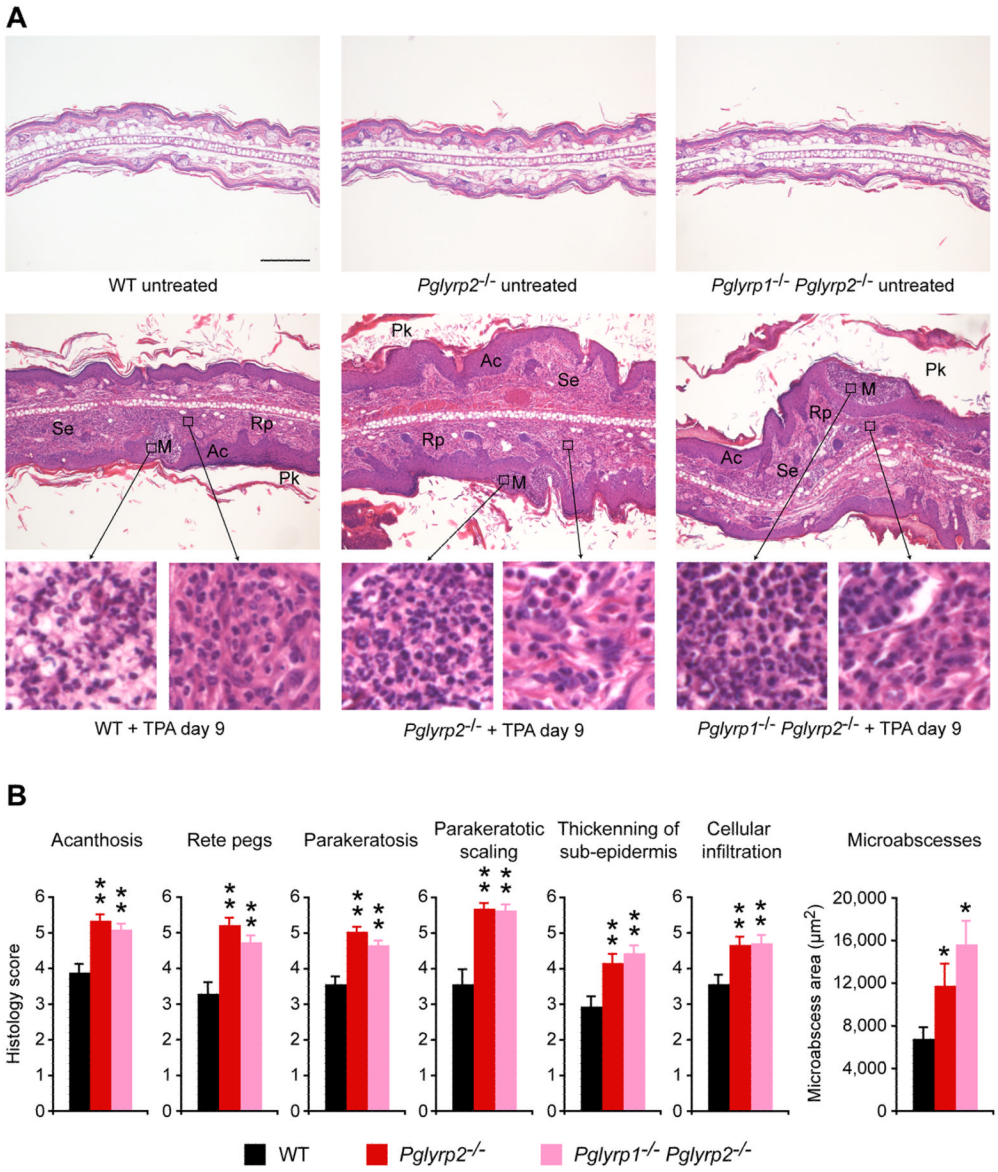

Figure 2. Ear histology in TPA-treated *Pglyrp2*$^{-/-}$ mice has many features of psoriasis

TPA application to the ears on days 0, 2, 4, 6, and 8 induced in *Pglyrp2*$^{-/-}$ mice acanthosis (Ac), formation of rete pegs (Rp), parakeratosis (Pk), parakeratotic scaling, formation of numerous epidermal microabscesses (M, primarily neutrophilic), and marked thickening of the sub-epidermal layer (Se) with dense cellular infiltrates (containing mainly PMNs and mononuclear cells), that were all highly prominent in *Pglyrp2*$^{-/-}$ mice and *Pglyrp1*$^{-/-}$*Pglyrp2*$^{-/-}$ mice, and less severe in WT mice. (**A**) H&E stained cross-sections at low magnification (large panels, bar = 200 μm) with high magnification insets. (**B**) Semi-quantitative evaluation of the extent of the indicated histologic changes and quantitative measurements of the surface areas of microabscesses on cross-sections of the ears; means ± SEM; N = 40 high power fields for histology scores and N = 78 to 123 microabscesses, all from 4 mice/group; significance of differences between *Pglyrp*$^{-/-}$ and WT mice: *, P<0.02; **, P<0.001.

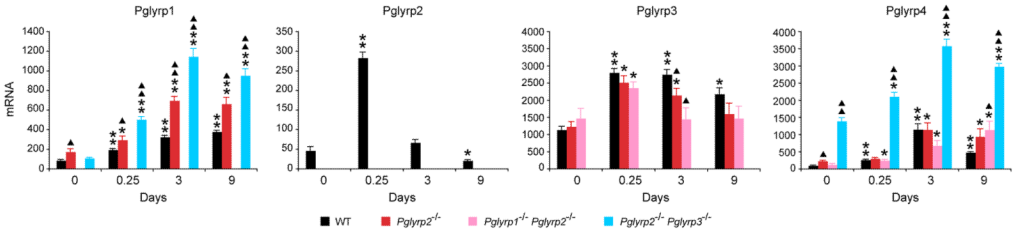

Figure 3. Pglyrp1, Pglyrp2, Pglyrp3, and Pglyrp4 expression is increased in the TPA-treated skin

The amounts of each PGRP mRNA in WT mice and in the indicated *Pglyrp*-deficient mice treated with TPA every other day were measured by qRT-PCR. The results are means of 3–4 mice ± SEM; *, P<0.04; **, P<0.001, treated versus untreated; ▲, P<0.04; ▲▲, P<0.001, *Pglyrp*$^{-/-}$ versus WT.

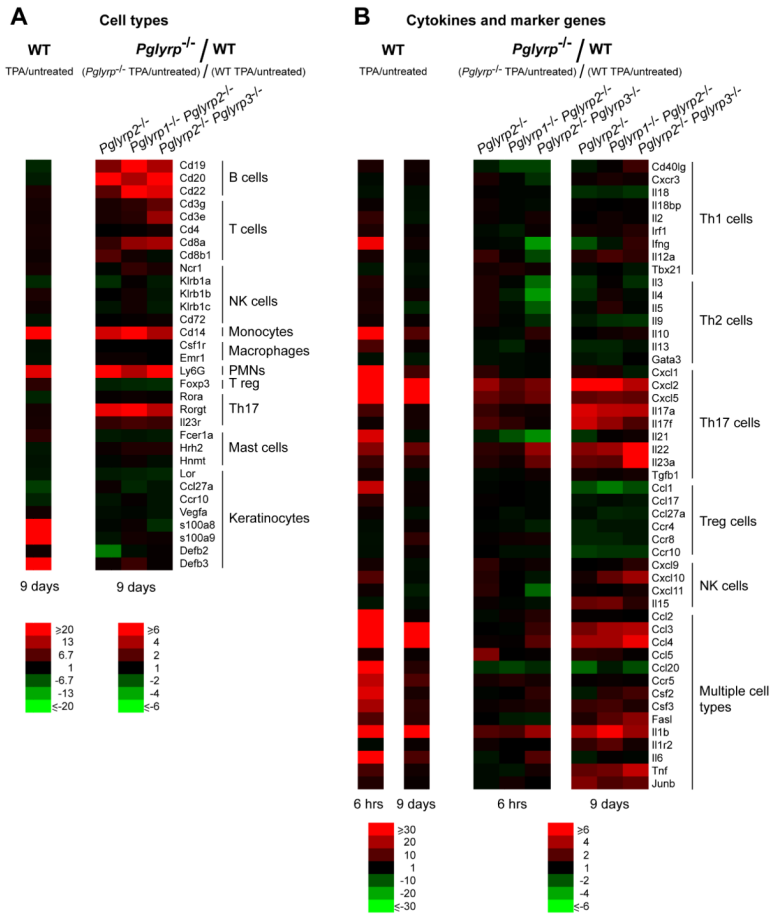

Figure 4. TPA-treated *Pglyrp2*$^{-/-}$ mice have increased PMNs, monocytes, B cells, and Th17 cells and a Th17-associated gene expression profile in the affected skin

Expression of a panel of (**A**) marker genes characteristic of various inflammatory cell types and (**B**) cytokines, chemokines, and other marker genes characteristic of Th1, Th2, Th17, Treg, NK, and other cell types in the ears of mice 6 hrs or 9 days after application of TPA to the ears on days 0, 2, 4, 6, and 8 measured by qRT-PCR. For WT mice (left panels), the ratio of the amount of mRNA in TPA-treated to untreated mice for each gene (fold induction by TPA) is shown; for *Pglyrp*$^{-/-}$mice, the results are the ratios of fold induction of each gene by TPA in *Pglyrp*$^{-/-}$ mice to fold induction of each gene by TPA in WT mice (which represents the fold difference in the response to TPA in *Pglyrp*$^{-/-}$ versus WT mice). The results are means of 3 arrays from 4–5 mice/group in heat map format. The means ± SEM bar graphs for these results are shown in Supplemental Figs 1-3.

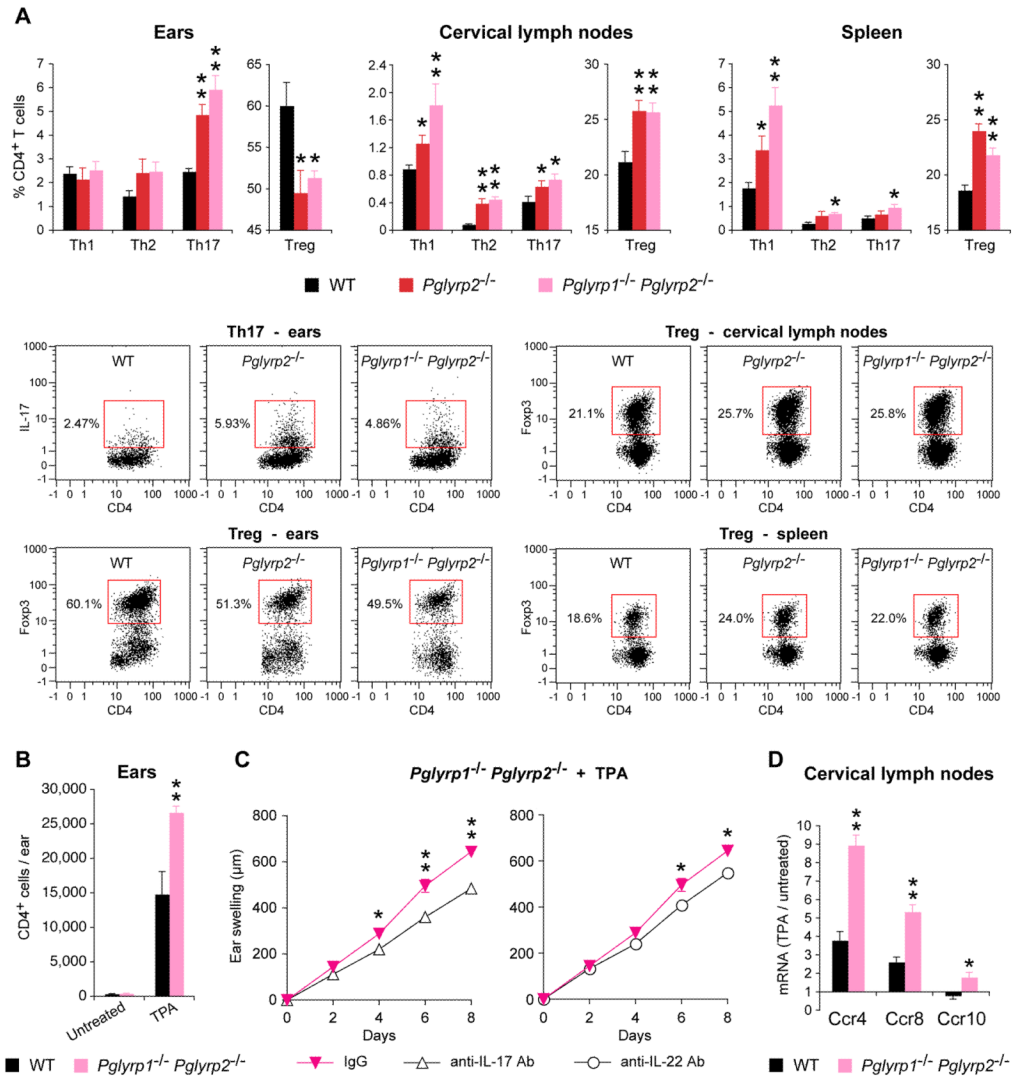

Figure 5. TPA-treated *Pglyrp2*$^{-/-}$ mice have high numbers of Th17 cells and low numbers of Treg cells in the affected skin, and IL-17 and IL-22 are required for the enhanced response to TPA in *Pglyrp2*$^{-/-}$ mice

(**A**) Percentages of Th1, Th2, Th17, and Treg cells in the ears, cervical lymph nodes, and spleen in WT, *Pglyrp2*$^{-/-}$ and *Pglyrp1*$^{-/-}$*Pglyrp2*$^{-/-}$ mice on day 9 after application of TPA to the ears on days 0, 2, 4, 6, and 8 measured by flow cytometry; means ± SEM of 5–9 mice/group (*, P<0.05; **, P<0.005; *Pglyrp*$^{-/-}$ versus WT) or representative dot plots for Th17 and Treg cells are shown; representative dot plots for Th1 and Th2 cells and isotype controls are shown in Supplemental Fig. 4. (**B**) Numbers of CD4^{+} cells in the untreated and TPA-treated (days 0, 2, 4, 6, and 8) ears of WT and *Pglyrp1*$^{-/-}$*Pglyrp2*$^{-/-}$ mice, means ± SEM; N = 4 mice/group; significance of differences between WT and *Pglyrp1*$^{-/-}$*Pglyrp2*$^{-/-}$ mice: **, P<0.005. (**C**) Ear swelling in *Pglyrp1*$^{-/-}$*Pglyrp2*$^{-/-}$ mice treated with TPA on days 0, 2, 4, and 6, and also treated with either isotype control IgG or neutralizing anti-IL-17 or anti-IL-22 mAbs; means ± SEM; N = 7 mice/group; significance of differences between IgG control and anti-IL-17 or anti-IL-22 mAbs-treated mice: *, P<0.05; **, P<0.005. (**D**) Expression of receptors for chemokines that attract Treg cells in cervical lymph nodes of WT and *Pglyrp1*$^{-/-}$*Pglyrp2*$^{-/-}$ mice on day 9 after application of TPA to the ears on days 0, 2, 4, 6, and 8 measured by qRT-PCR; the ratio of the amount of mRNA in TPA-treated to

untreated mice for each gene (fold induction by TPA) is shown as means ± SEM of 3 arrays from 5 mice/group (*, P<0.05; **, P<0.005; *Pglyrp*$^{-/-}$versus WT).

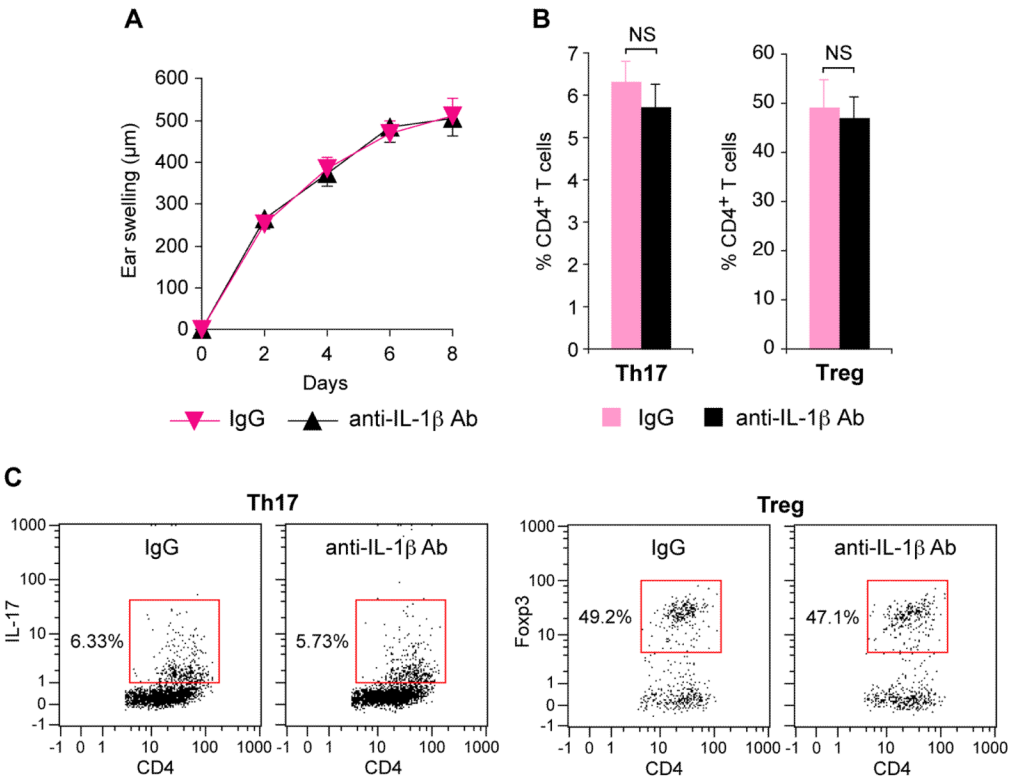

Figure 6. IL-1β is not responsible for greater inflammation, increased numbers of Th17 cells and decreased numbers of Treg cells in the skin of TPA-treated *Pglyrp1*$^{-/-}$*Pglyrp2*$^{-/-}$ mice

(**A**) Ear swelling in *Pglyrp1*$^{-/-}$*Pglyrp2*$^{-/-}$ mice treated with TPA on days 0, 2, 4, and 6, and also treated with either isotype control IgG or neutralizing anti-IL-1β mAbs; means ± SEM. (**B**) Percentages of Th17 and Treg cells in the ears of *Pglyrp1*$^{-/-}$*Pglyrp2*$^{-/-}$ mice on day 9 after application of TPA to the ears on days 0, 2, 4, 6, and 8 measured by flow cytometry; means ± SEM. (**C**) Representative dot plots for Th17 and Treg cells. N = 7 mice/group; all differences between IgG control and anti-IL-1β mAbs-treated mice were not significant (NS, P>0.05).